Vol.66(spe): e23230078, 2023
https://doi.org/10.1590/1678-4324-ssbfar-2023230078
ISSN 1678-4324 Online Edition
II South-Brazilian Symposium on Pharmacognosy

*Article - Health Science/Pharmacognosy*

# Applications of Calcium Oxalate Crystal Microscopy in the Characterization of *Baccharis articulata*

**Paola Aparecida Raeski**[1*]
https://orcid.org/0000-0002-8481-4612

**Gabrielly de Oliveira Ayres**[2]
https://orcid.org/0000-0001-5480-079X

**Luciane Mendes Monteiro**[1]
https://orcid.org/0000-0003-2896-8147

**Gustavo Heiden**[3]
https://orcid.org/0000-0002-0046-6500

**Andressa Novatski**[4]
https://orcid.org/0000-0002-8327-6285

**Vijayasankar Raman**[5]
https://orcid.org/0000-0001-7368-9644

**Ikhlas Ahmed Khan**[5]
https://orcid.org/0000-0001-5464-4643

**Emerson Luiz Botelho Lourenço**[6]
https://orcid.org/0000-0002-1798-7871

**Arquimedes Gasparotto Junior**[7]
https://orcid.org/0000-0003-3433-5098

**Paulo Vitor Farago**[1]
https://orcid.org/0000-0002-9934-4027

**Jane Manfron**[1]
https://orcid.org/0000-0003-1873-2253

[1]Universidade Estadual de Ponta Grossa, Programa de Pós-graduação em Ciências Farmacêuticas, Ponta Grossa, Paraná, Brasil; [2]Universidade Estadual de Ponta Grossa, Departamento de Ciências Farmacêuticas, Ponta Grossa, Paraná, Brasil; [3]Embrapa Clima Temperado, Pelotas, Rio Grande do Sul, Brasil; [4]Universidade Estadual de Ponta Grossa, Programa de Pós-graduação em Ciências da Saúde, Ponta Grossa, Paraná, Brasil; [5]National Center for Natural Products Research, University of Mississippi, University, MS, USA; [6]Universidade Paranaense, Laboratório de Pesquisa Pré-clínica de Produtos Naturais, Umuarama, Paraná, Brasil; [7]Universidade Federal da Grande Dourados, Laboratório de Eletrofisiologia e Farmacologia Cardiovascular, Dourados, Mato Grosso do Sul, Brasil.

Editor-in-Chief: Yasmine Mendes Pupo
Associate Editor: Sinvaldo Baglie

Received: 24-Jan-2023; Accepted: 25-May-2023

*Correspondence: paola.ap.raeski@gmail.com; Tel.: +55-42-3220-3124

**HIGHLIGHTS**

- Eleven crystalline morphotypes were found in *Baccharis articulata*.
- Calcium oxalate is the chemical composition of the crystals.
- Both monohydrate and dihydrate types were found in *B. articulata* crystals.
- Crystal morphotypes can be used as anatomical markers.

**Abstract:** *Baccharis articulata* (Lam.) Pers., popularly known as carqueja, carquejinha or carqueja-doce, is a plant widely used in traditional medicine as a diuretic, digestive and antidiabetic. Due to its similar morphology with other species of the "carqueja group", especially *Baccharis pentaptera* (Less.) DC., it can be easily confused even by specialists. Thus, this study aimed to characterize micromorphology of the crystals present in *B. articulata* to show botanical markers that can help differentiate this species from other

carquejas. Eleven crystalline morphotypes, including druses, styloids and various shapes of prismatic and sand crystals, were evidenced by scanning electron microscopy. In addition, the elemental chemical composition and the degree of hydration of the crystals were analyzed by EDS and Raman spectroscopy. The results of this study would aid in the authentication of *B. articulata* and serve as a basis for future studies of other species of *Baccharis*.

**Keywords:** Anatomy; *Baccharis*; Carqueja; Raman spectroscopy; Energy dispersive X-ray spectroscopy; Polarization light microscopy; Scanning electron microscopy; Crystals; Calcium oxalate.

## INTRODUCTION

The genus *Baccharis* L. comprises about 440 species, distributed from Canada to the southern region of South America, with 179 species occurring in Brazil [1,2]. This genus is economically important, and many species are widely used in folk medicine [3]. Among the most important species, *Baccharis articulata* (Lam.) Pers., popularly known as carqueja, carquejinha, or carqueja-doce, is widely used as a digestive and diuretic medicine in the southern regions of Brazil, Uruguay and Argentina, and as an antidiabetic in Paraguay [4]. It is a shrubby species, with erect stems and branches that are light green to grayish-green and have two wing-like expansions. The cladodes are sessile, obovate in shape and obtuse at the apex [5]. It can be easily confused with other carqueja species, as is the case of *Baccharis pentaptera* (Less.) DC., which has two winged expansions in the apical portions of the branches [6, 7]. Considering the confusion due to the morphological similarities, similar therapeutic uses and same folk names applied to different species, this study aimed to provide microscopic and taxonomic data to support the characterization and authentication of the carquejas complex.

## MATERIAL AND METHODS

### Plant Material

Vegetative aerial parts of *B. articulata* were collected in November 2009, in the region of Turuçu, Rio Grande do Sul and deposited in the Herbarium Clima Temperado of Embrapa Clima Temperado, under registration number ECT 154, and in June 2022 in the Metropolitan region of Curitiba and deposited in the Herbarium of the State University of Ponta Grossa (UEPG), under registration number HUPG 20595. Access to genetic heritage was authorized and licensed by the National System for the Management of Genetic Heritage and Associated Traditional Knowledge (SisGen) and is under the code AFEEC2B.

After collection, the cladodes were fixed in FAA 70 solution (formalin, acetic acid and alcohol) for three days, washed with water and stored in 70% alcohol [6].

### Light Microscopy (LM)

Cross sections of cladodes of *B. articulata* were stained with Astra blue and basic fuchsin [9], placed on glass slides with 50% glycerin [10], covered with a glass slide and glazed with a transparent base for luting.

### Polarization light microscopy (PL)

The samples were kept in sodium hypochlorite solution for 12 h, or until they became translucent. Then they were washed with distilled water, neutralized with 5% acetic acid [11] and stained with safranin. The slides were mounted with glycerin (50%) and photomicrographs were taken using a Nikon E600 POL polarized microscope equipped with a Nikon DSFiv camera system and Nikon Elements imaging software at the National Center of Natural Products Research (NCNPR), University of Mississippi, USA.

### Scanning electron microscopy (SEM)

The cross sections made for SEM were dehydrated in a series of ethanol solutions of increasing concentrations and then dried in a critical point dryer [12]. The dried samples were mounted on aluminum stubs and coated with gold in a Quorum SC 7620 sputter coater. The samples were analyzed and imaged in a Mira 3 Teskan SEM in high vacuum mode with an accelerating voltage of 15 kV located in the Multi-users Laboratory Complex (C-LABMU) at UEPG.

## Energy dispersive X-ray spectroscopy (EDS)

The analyses concerning the elemental chemical composition of the crystals were performed using EDS, conducted in cells containing crystals and in empty cells for control [13]. The samples were subjected to an X-ray detector coupled to the SEM maintained under the same operating conditions used to capture the electromicrographs.

## Raman spectroscopy (RS)

The hydration state of the crystals was observed using an Horiba LabRAM HR Evolution spectrometer with an excitation laser of 785 nm wavelength, 300 lines/mm grids, Synapse detector coupled to an optical microscope located in the laboratory of nanophotonics and imaging at the Federal University of Alagoas (UFAL). For each measurement, 30 averages were taken with an exposure time of 15 s,in the range of 100 to 1600 $cm^{-1}$ [14, 15].

## RESULTS

Eleven crystalline morphotypes were found in *B. articulata* using transmitted and polarized light microscopy (Figures 1 a-f; 4 c-f). The crystal micromorphologies were also evaluated and described using the SEM (Figures 2 a-h; 3 a-l; 4 a, b; 5 a-f). The crystal morphotypes found in the epidermis and glandular trichomes of cladodes are bipyramidal simple (Figure 2 a, b, d), bipyramidal rectangular (Figure 2 c, e, g), pyramidal rectangular (Figure 2 f, h), cuneiform (Figure 3 a, b), styloid (Figure 3 a, c, d, e), rhomboid (figure 3 h, i), arrow-shaped (Figure 3 f, g), druse (Figure 4 a-f), crystalline sand rounded (Figure 5 a, b), crystalline sand styloid (Figure 5 c, d) and crystalline sand bow-tie-shaped (Figure 5 e, f). The definitions of the micromorphologies and their locations are summarized in Table 1.

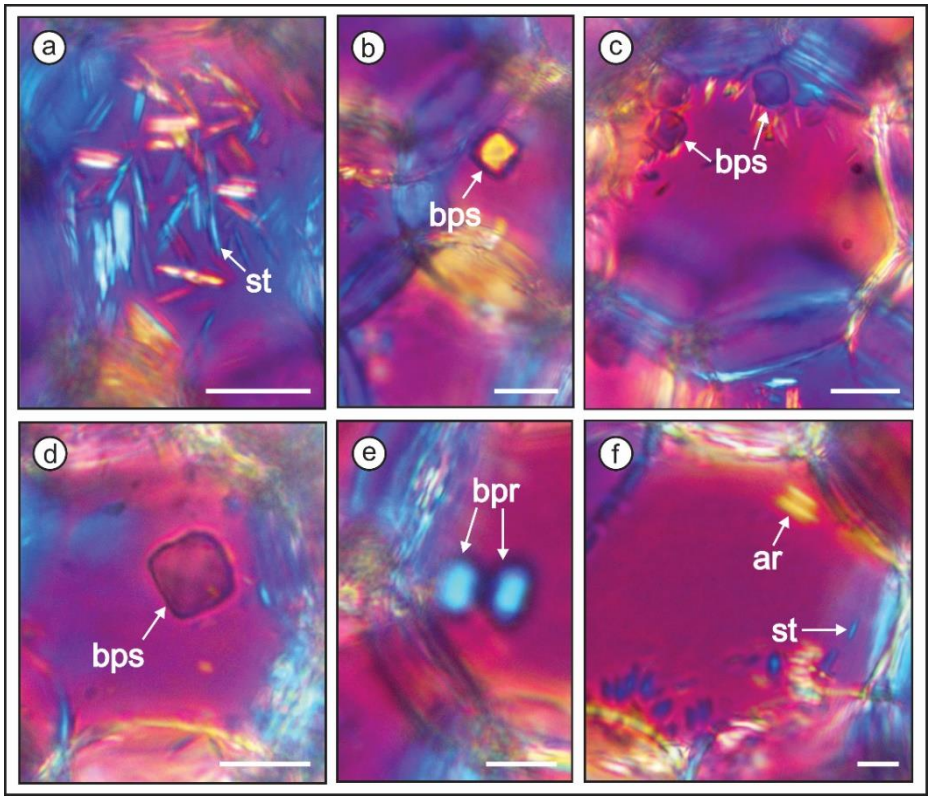


**Figure 1.** Cross-section of *Baccharis* articulata stem showing crystals under polarized light microscopy (a-f) [st - styloid crystal; bps - bipyramidal simple crystal, bpr - bipyramidal rectangular crystal; ar - arrow shaped] Scale bars: a-d = 10 µm; e-f = 5 µm.

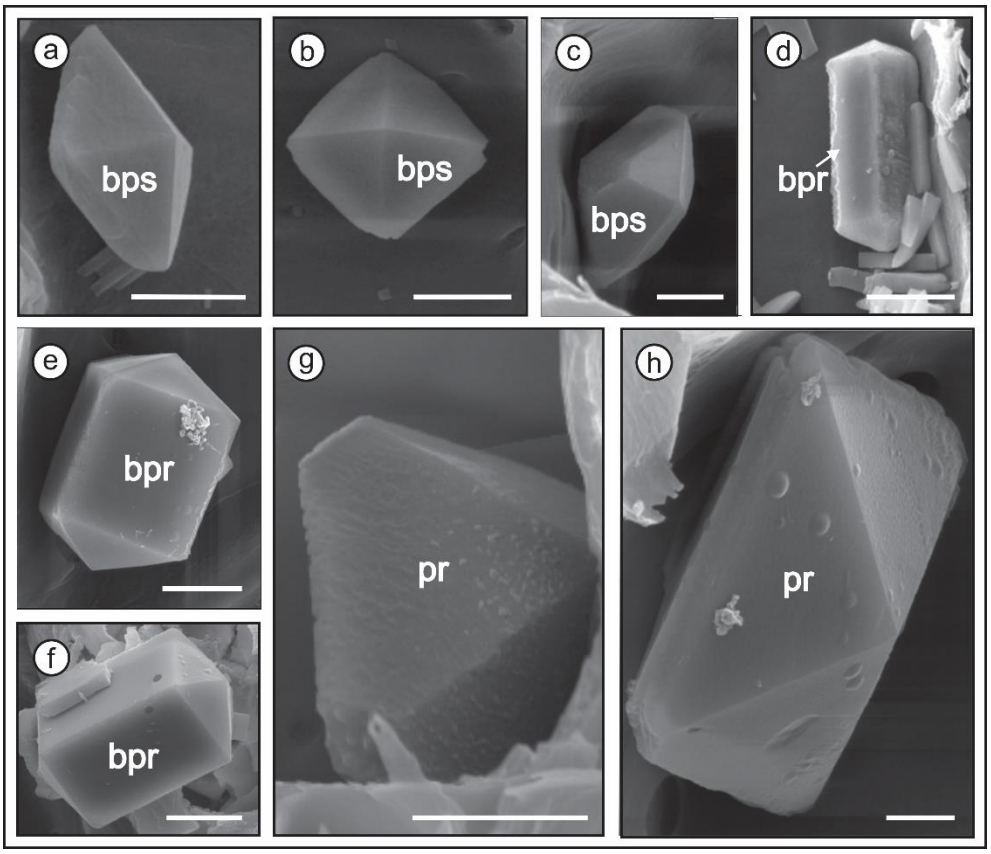


**Figure 2.** SEM images of the tetragonal crystal system found in *Baccharis articulata* stems [SEM (a-f)] [bps - bipyramidal simple; bpr - bipyramidal rectangular; pr - pyramidal rectangular] Scale bars: a = 10 µm; b-g = 5 µm; h = 2µm.

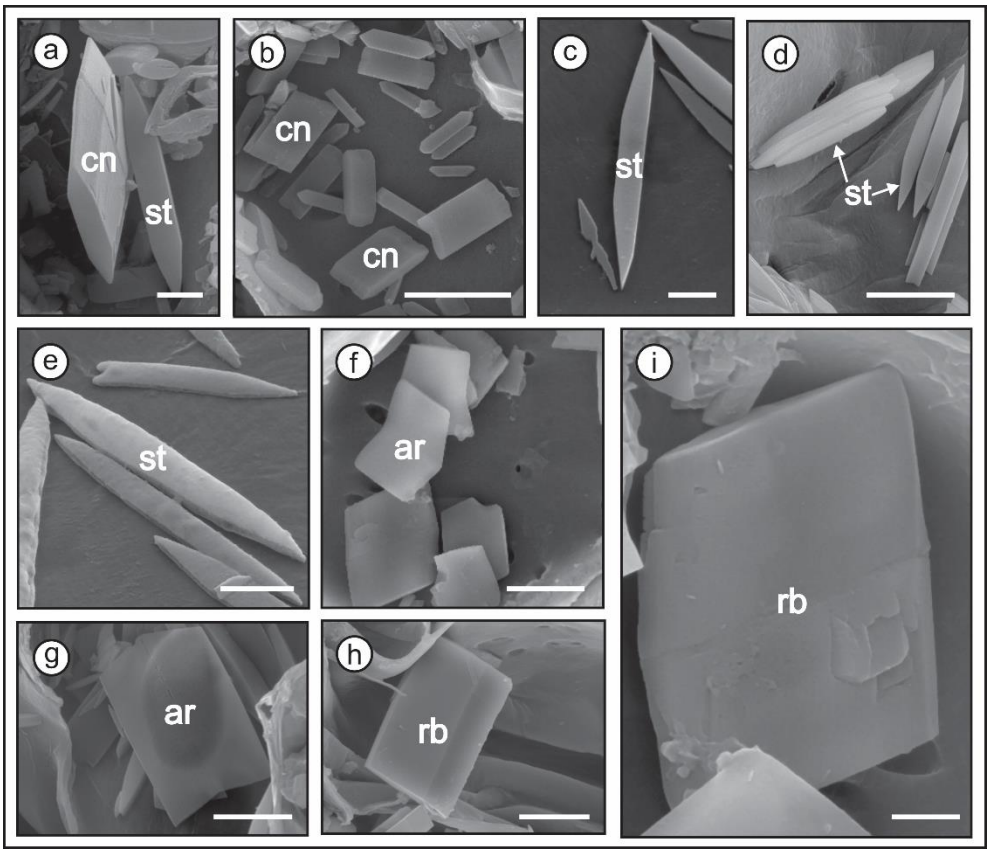


**Figure 3.** SEM images of monoclinic crystal system found in *Baccharis articulata* stems (a-i)] [cn - cuneiform; st - styloid; ar - arrow-shaped; rb - rhomboid] Scale bars: a, c, e, i = 2µm; d, f-h = 5 µm; b = 10 µm.

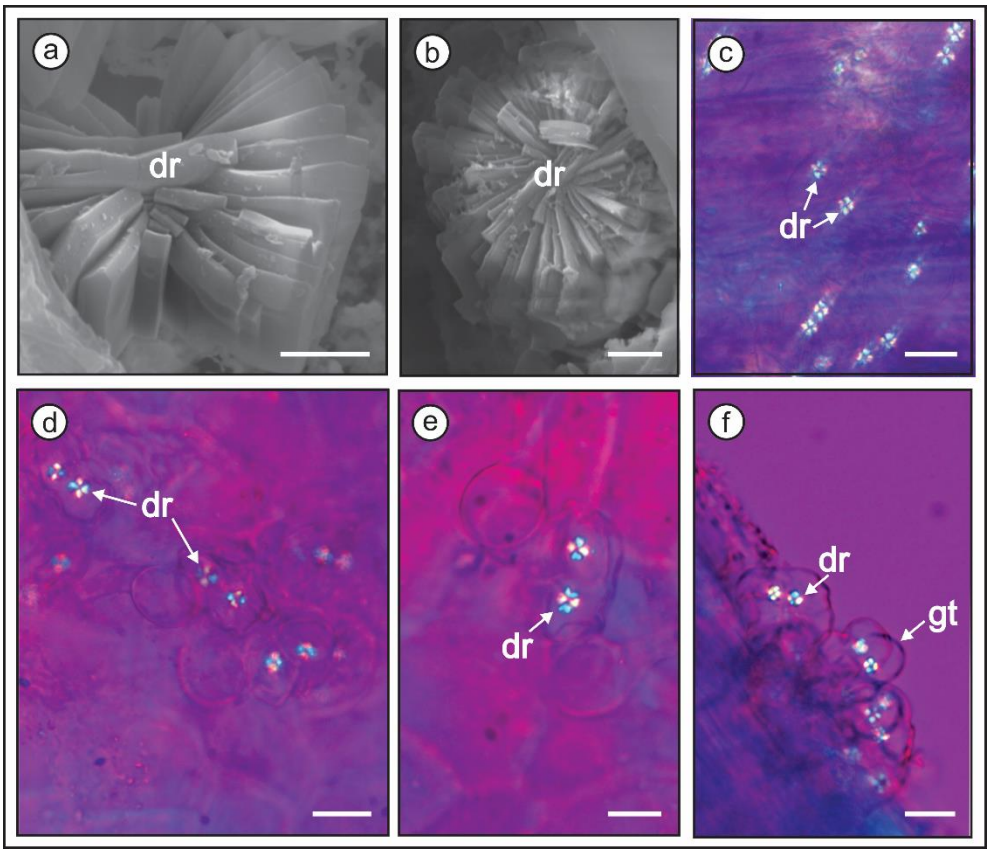


**Figure 4.** Druses found in *Baccharis articulata* stem (a-b), leaf epidermis (c), and glandular trichomes (d-f) [SEM (a-b); LP (c-f)] [dr - druse; gt - glandular trichome] Scale bars: a-b = 2µm; c-f = 20 µm.

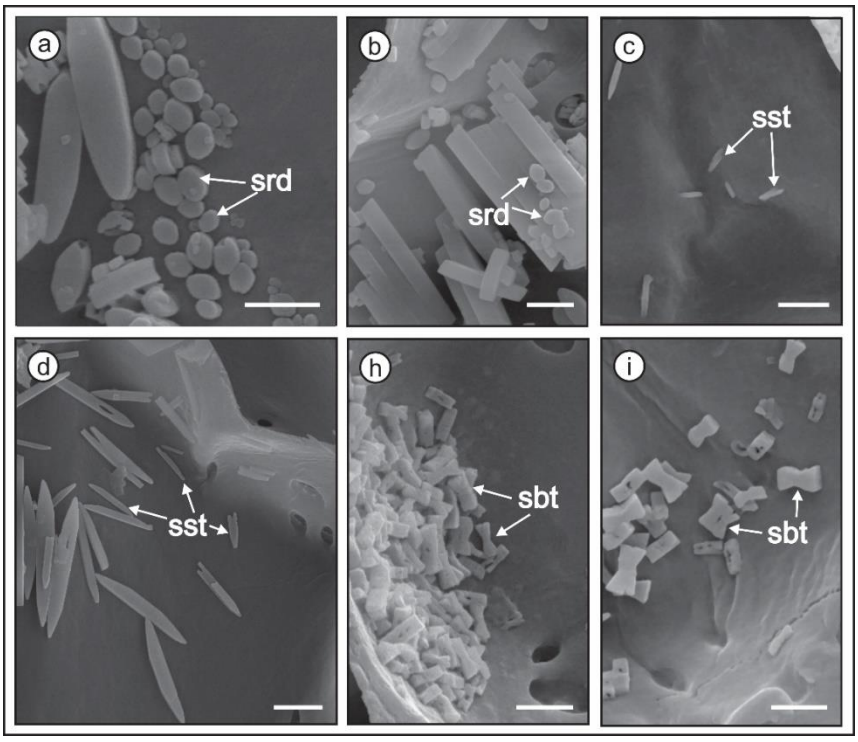


**Figure 5.** SEM images of the crystalline sand found in *Baccharis articulata* stems (a-f)] [srd - crystalline sand rounded; sst - crystalline sand styloid; sbt - crystalline sand bow-tie-shaped]. Scale bars: a, b, e, f = 2µm; c, d = 5 µm.

**Table 1.** Crystal Morphotypes Observed in *B. articulata*: Definition and Location in the Species

| | Morphotype | Definition | Location |
|---|---|---|---|
| Tetragonal crystal system | Bipyramidal simple | Crystals characterized by the direct union of two pyramids [16, 17]. | Stem |
| | Bipyramidal rectangular | Crystals with a considerably thick, rectangle base, which connects the two pyramids at the ends [17, 18]. | Stem |
| | Pyramidal rectangular | They are presented as a pyramid with a rectangle-shaped base [16]. | Stem |
| | Cuneiform | Crystals resembling a rectangular prism with tapered ends. They got this term because they resemble a wedge [13]. | Stem |
| | Druse | Spherical aggregate of crystals, individually deposited, which can take different shapes (Rhomboidal, styloid) [19, 20]. | Stem, epidermis and apical cells of the glandular trichome |
| Monoclinic crystal system | Styloid | They appear as elongated crystals, with pointed ends in frontal view, or truncated on the lateral face [19, 21]. | Stem, epidermis |
| | Rhomboidal | Parallelogram with unequal adjacent sides [13]. | Stem |
| | Arrow shaped | It is characterized by having a pointed end and the opposite end with a "V" shaped indentation, resembling the tip of an arrow [22]. | Stem |
| | Crystalline sand rounded | Portrayed as a mass of small individual crystals, smaller than 3 µm. They can be of various shapes, as shown here: rounded, styloid and bow-tie-shaped [19]. | Stem |
| | Crystalline sand styloid | | |
| | Crystalline sand bow-tie-shaped | | |

In *B. articulata*, the presence of calcium, carbon and oxygen in a 1:2:4 ratio evidenced the chemical composition of calcium oxalate for the analyzed crystals. Figure 6 (b-f) exemplifies the peaks found in some crystals. As a negative control, an empty cell was tested, showing only carbon and oxygen peaks representing the elements of the natural chemical composition of the cell, ensuring the reliability of the analysis (figure 6 a).

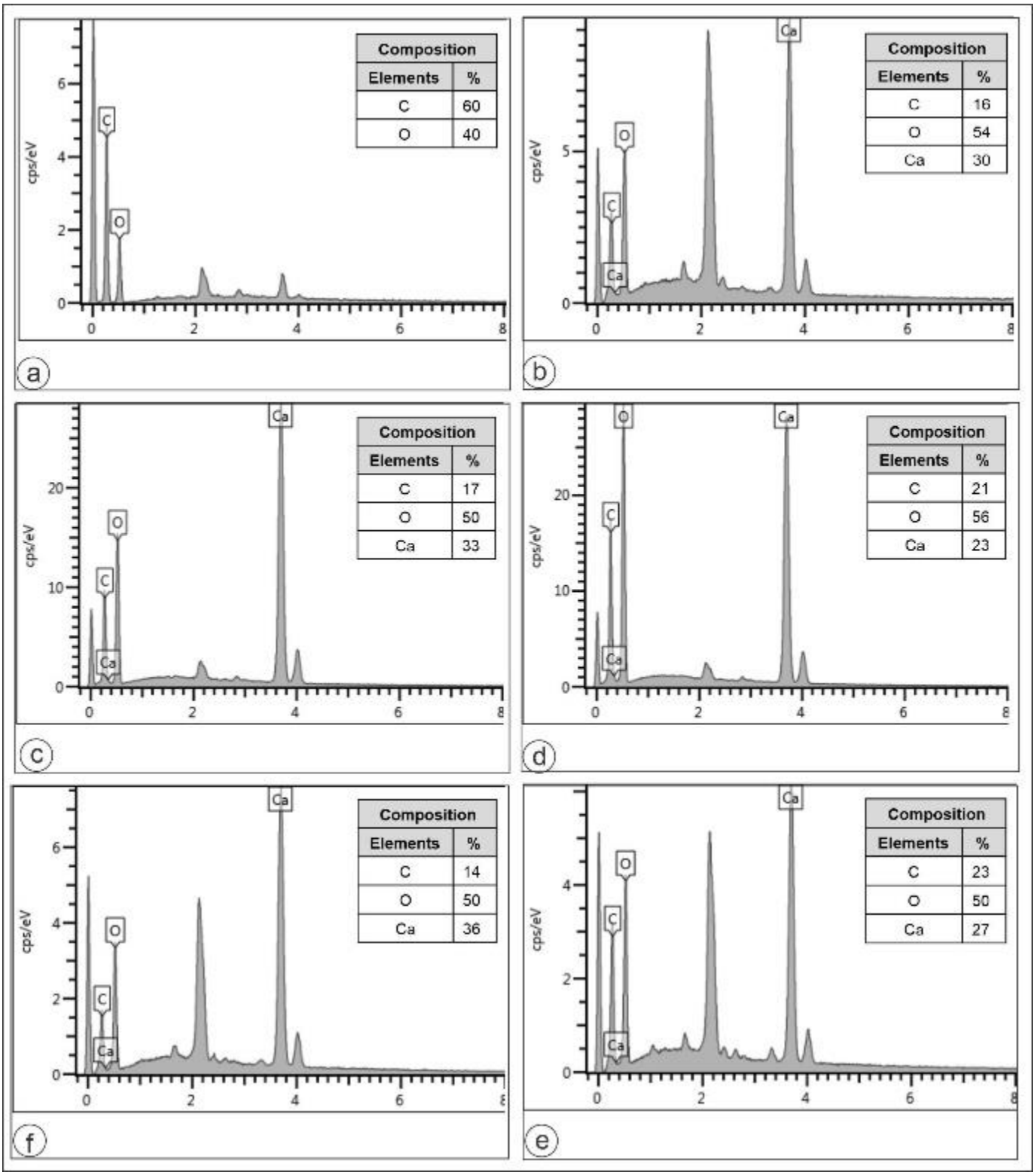


**Figure 6**. EDS of the crystals found in *Baccharis articulata*. [a - EDS of cell devoid of crystals as control; b-c - EDS of bipyramidal rectangular crystal; d-e - EDS of pyramidal rectangular crystal; f - EDS of arrow-shaped crystal. The prominent unlabeled peak near 2 keV represents gold (Au), the metal used to sputter-coat the samples].

Both hydration states were observed in *B. articulata*; the dihydrate state identified in bipyramidal (figure 7 a, b) and pyramidal crystals, while the monohydrate state in styloid (figure 7 c,d), cuneiform, druse, rhomboid and arrow-shaped crystals. The sand crystals, on the other hand, could not be analyzed by the equipment due to their size being less than 5 µm.

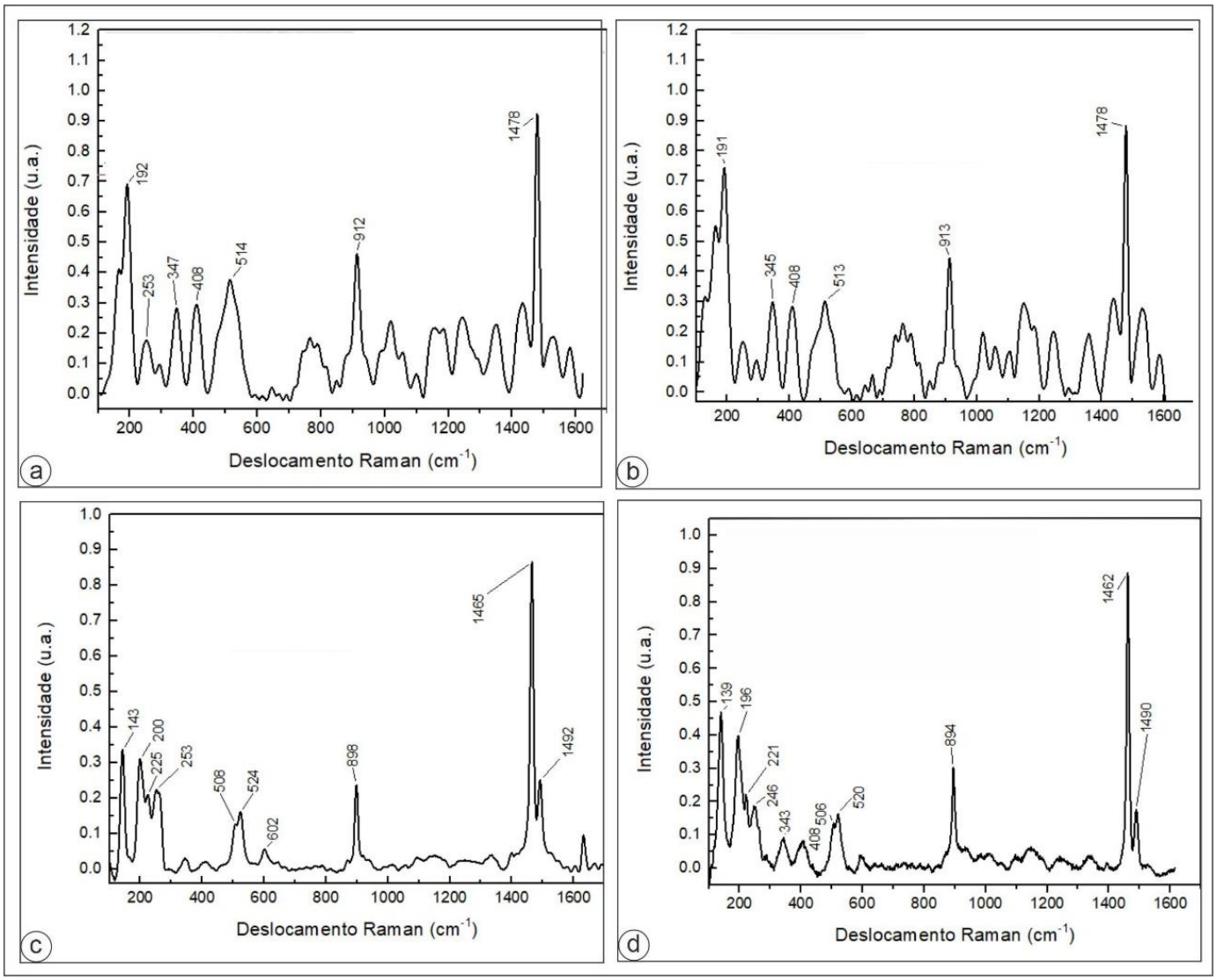


**Figure 7.** Raman spectroscopy of crystals found in *Baccharis articulata*. a, b - dihydrate bipyramidal simple crystals (weddellite); c, d - monohydrate styloid crystals (whewellite).

## DISCUSSION

The production of inorganic crystals can vary considerably in their morphology from species to species. From the point of view of genetics, a particular species may produce a specific type of crystal, or even a subset of different crystals and this may differentiate it from other species in the genus [23]. As well as morphology, genetics can act on the location of the crystal morphotype in the plant, varying considerably from species to species [23, 24]. As the genus *Baccharis* has many similar species [25-27], the more anatomical markers described in the literature, the easier the identification of these species will be. Thus, the eleven crystalline morphotypes observed in *B. articulata* act as a subset of different crystals observed in the species, and will serve as anatomical markers to distinguish it from other species in the genus.

Besides genetic control, the proportion of calcium, or even the presence of contaminating substances, such as heavy metals, can influence the determination of crystal morphology [23]. In general, the chemical composition of the crystals may vary depending on the soil in which the plant is found. The presence of compounds such as sodium, potassium, calcium, aluminum, copper and sulfate can alter the development of crystalline morphotypes [28, 29]. Chemically, the formation of these crystals occurs from endogenously synthesized oxalic acid ($C_2H_2O_4$). In general, the most commonly found chemical form crystals in plants is calcium oxalate ($CaC_2O_4$), but other forms can also appear, such as calcium carbonate ($CaCO_3$) [28].

Recently, studies on various plants have evidenced the chemical composition of crystals by EDS which show a predominance of calcium oxalate crystals in the species [30-33]. These crystals appear in more than 215 distinct botanical families, and are distributed in almost all plant organs and tissues, from stems to roots, leaf structures, and seeds. In most cases, they have well-defined shapes, except when they have other contaminants in their structures, and can assume an amorphous form [19].

In addition to the chemical composition, the hydration state of the crystals can significantly influence the development of their morphology. There are two states of hydration that are commonly found, which are the monohydrate form (whewellite) and the dihydrate form (weddellite), which are dependent on the concentration of calcium present in the plant for their formation [19, 21].

The monohydrate form generally occurs in monoclinic crystal sistem, which are crystals that have three different length axes, such as styloid crystals, while the dihydrate form comprises crystals that are part of the tetragonal system, which are characterized by having three mutually perpendicular axes, such as bipyramidal, pyramidal, and prismatic crystals. In *B. articulata*, this correlation between the hydration state and the morphology of the crystals can be observed. Even though this correlation influences the development of some crystalline forms, others may present both states of hydration, as in the case of druses, which may present either monohydrate or dihydrate form [23, 34, 35].

Until recently, the presence of crystals in plant species was not considered a marker for species differentiation. Currently, although the mechanism of genetic control, chemical regulation and hydration in crystal formation are not clearly defined, it is known that there is strict genetic control in play and each species can produce a crystalline morphotype or a subset of morphotypes. In the case of *B. articulata*, the set of crystal morphotypes found can help in the morphoanatomical characterization of the species and help differentiate it from others. This study would also form a basis for future research involving other species of *Baccharis*.

## CONCLUSION

Four major types of calcium oxalate crystals (druses, prisms, styloids and sand crystals) with eleven morphotypes were observed in *B. articulata* stems and cladodes. The prismatic crystals were observed in the forms of bipyramidal (simple and rectangular), pyramidal rectangular, cuneiform, tabular, and arrow-shaped. Crystalline sands with three shapes of individual crystals such as rounded, styloid, and bow-tie-shaped, were observed in the stems. Styloids were observed both in the stems and cladodes, while druses were found in the apical cells of the glandular trichomes, stems and cladodes. Bipyramidal and pyramidal crystals were dihydrated, and styloid crystals were monohydrated.

The present study provides additional micromorphological characteristics to those previously described in the literature for *B. articulata* and can be used as anatomical markers, serving as a basis for future studies of the species of the "carqueja complex" of *Baccharis*.

**Funding:** This research was funded by CAPES, grant number 88887.634811/2021.
**Acknowledgments:** To UEPG, C-LABMU and UFAL. GH acknowledges CNPq PQ2 314590/2020-0.
**Conflicts of Interest:** The funders had no role in the design of the study; in the collection, analyses, or interpretation of data; in the writing of the manuscript, or in the decision to publish the results.

## REFERENCES

1. Heiden G, Antonelli A, Pirani, AAJR. A novel phylogenetic infrageneric classification of *Baccharis* (Asteraceae: Astereae), a highly diversified American genus. Taxon. 2019;58(5):1048-81.
2. Heiden G. *Baccharis*. Flora e Funga do Brasil [Internet]. Rio de Janeiro: JBRJ; 2022 [cited 2022 oct]. Available from: https://floradobrasil.jbrj.gov.br/FB5151.
3. Budel JM, Wang M, Raman V, Zhao J, Khan SI, Rehman JU, et al. Essential oils of five *Baccharis* Species: investigations on the chemical composition and biological activities. Molecules. 2018;23(10):1-19.
4. Abad MJ, Bermejo P. *Baccharis* (Compositae): a review update. Arkivoc. 2007;2(7):76-96.
5. Heiden G, Iganci JRV, Macias L. *Baccharis* sect. *Caulopterae* (Asteraceae, Astereae) no Rio Grande do Sul, Brasil [Baccharis sect. Caulopterae (Asteraceae, Astereae) in Rio Grande do Sul, Brazil]. Rodriguesia. 2009;60(4):943-83.
6. Budel JM, Paula JPDe, Santos VLPDos, Franco CRC, Farago PV, Duarte MR. Pharmacobotanical study of *Baccharis pentaptera*. Rev. Bras. Farmacogn. 2015;25(4):314-9.
7. Duarte MR, Budel JM. Análise morfoanatômica comparativa de duas espécies de carqueja: *Baccharis microcephala* DC. e *B. trimera* (Less.) DC., Asteraceae. [Comparative morphoanatomical analysis of two carqueja species: *Baccharis microcephala* DC. and *B. trimera* (Less.) DC., Asteraceae]. Braz. J. Pharm. Sci. 2009;45(1):75-85.
8. Johansen DA. Plant microtechnique. 1st ed. New York: McGraw-Hill Books; 1940. 530 p.
9. Kraus JE, Sousa HC, Rezende MH, Castro NM, Vecchi C, Luque R. Astra Blue and Basic Fuchsin Doublé Staining of Plant Materials. Biotech Histochem. 1998;73(5):235-43.
10. Berlyn GP, Miksche JP. Botanical microtechnique and cytochemistry. 1st ed. Ames: Iowa State University; 1976. 326 p.
11. Shobe WR, Lersten NR. A technique for clearing and staining Gymnosperm leaves. Bot. Gaz. 1998;128(2):150-2.

12. Souza W. Técnicas básicas de microscopia eletrônica aplicadas às Ciências Biológicas [Basic electron microscopy techniques applied to Biological Sciences]. 1st ed. Rio de Janeiro: Sociedade Brasileira de Microscopia Eletrônica; 1998. 179p.
13. Machado CD, Raman V, Rehman JU. Maia, B. H.; Meneghetti, E. K. *Schinus molle*: anatomy of leaves and stems, chemical composition and insecticidal activities of volatile oil against bed bug (*Cimex lectularius*). Rev. Bras. Farmacogn. 2019;29(1):1-10.
14. Edwards HGM, Farwell DW, Jenkins R, Seaward MRD. Vibrational Raman spectroscopic studies of calcium oxalate monohydrate and dihydrate in lichen encrustations on renaissance frescoes. J. Raman Spectrosc. 1992;23(3):185-9.
15. Frost RL. Raman spectroscopy of natural oxalates. Anal. Chim. Acta. 2004;517(1-2):207-14.
16. Chvátal M. Cristalografia: Mineralogia para principiantes [Crystallography: Mineralogy for beginners]. 1st ed. Rio de Janeiro: Sociedade Brasileira de Geologia; 2007. 232 p.
17. Uloth MB, Clode PL, You MP, Barbetti MJ. Calcium oxalate crystals: An integral component of the *Sclerotinia sclerotiorum*/ *Brassia carinata* Pathosystem. PLoS One. 2015;10(3):1-15.
18. Sun XY, Ouyang JM, Zhu WY, Li YB, Gan QZ. Size-dependent toxicity and interactions of calcium oxalate dihydrate crystals on vero renal epithelias cells. J. Mater. Chem. B. 2015;3(1):1864-78.
19. Franceschi VR, Horner HT. Calcium oxalate crystals in plants. Bot. Rev. 1980;46(4):361-16.
20. He H, Bleby TM, Vaneklaas EJ, Lambers H, Kuo J. Morphologies and elemental compositions of calcium crystal in phyllodes and branchlets of *Acacia robeorum* (Leguminosae: Mimosideae). Ann. Bot. 2012;109(5):887-96.
21. Raman V, Horner HT, Khan IA. New and unusual forms of calcium oxalate raphide crystals in the plant kingdom. J. Plant Res. 2014;127(6):721-30.
22. Raeski PA, Heiden G, Novatski A, Raman V, Khan IA, Manfron J. Calcium oxalate crystal macropattern and its usefulness in the taxonomy of *Baccharis* (Asteraceae). Microsc. Res. Tech. 2023;86(7):862-81.
23. Franceschi VR, Nakata PA. Calcium oxalate in plants: Formation and function. Annu. Rev. Plant Biol. 2005;5(1)6:41-71.
24. Al-Rais AH, Myers A, Watson L. The isolation and properties of oxalate crystals from plants. Ann. Bot. 1971;35(1):1213-18.
25. Duarte MR, Budel JM. Estudo farmacobotânico de folha e caule de *Baccharis uncinella* DC., Asteraceae [Pharmacobotanical study of leaf and stem of *Baccharis uncinella* DC., Asteraceae]. Lat. Am. J. Pharm. 2008;28(1):740-6.
26. Budel JM, Duarte MR, Farago PV, Franco CRC, Santos VLP, Oliveira A. Comparative morpho-anatomical study of *Baccharis curitybensis* Heering ex Malme and *Baccharis spicata* (Lam.) Baill. Lat. Am. J. Pharm. 2011;30(8):1560-6.
27. Budel JM, Duarte MR, Santos CAM. Caracteres morfo-anatômicos de *Baccharis gaudichaudiana* DC., Asteraceae. Acta Farm. Bonaer. 2003;22(4):313-20.
28. Bosqueiro ALD. Metabólitos Secundários Em Plantas [Secondary Metabolites In Plants]. Ciênc. Educ. 1995;13(2):91-6.
29. Webb MA. Cell-mediated crystallization of calcium oxalate in plants. Plant Cell. 1999;11(1):751-761.
30. Lerstern NR, Horner HT. Crystal macropattern development in *Prunus Serotina* (Rosaceae, Prunoideae) leaves. Ann. Bot. 2006;97(1):723-9.
31. De Brito PS, Sabedotti C, Flores TB, Raman V, Bussade JE, Farago PV, Manfron J. Light and scanning electron microscopy, energy dispersive X-ray spectroscopy, and histochemistry of *Eucalyptus tereticornis*. Microsc. Microanal. 2021;27(5)1-9.
32. Almeida VP, Raman V, Raeski PA, Urban AM, Swiech JN, Miguel MD, Farago PV, Khan IA, Budel JM. Anatomy, micromorphology, and histochemistry of leaves and stems of *Cantinoa althaeifolia* (Lamiaceae). Microsc. Res. Tech. 2020; 83(5):551-7.
33. Pauzer MS, Borsato TO, Almeida VP, Raman V, Justus B, Pereira CB, Flores TB, Maia BHNS, Meneguetti E, Kanunfre CC, Paula JFP, Farago PV, Budel JM. *Eucalyptus cinerea*: Microscopic profile, chemical composition of essential oil and its antioxidant, microbiological and cytotoxic activities. Braz. Arch. Biol. Technol. 2021;64(spe):1-19.
34. Lepage L, Tawashi R. Growth and characterization of calcium oxalate dihydrate crystal (weddellite). J. Pharm. Sci. 1982;71(9):1059-62.
35. Ishii Y. Three kinds of calcium oxalate hydrates. Nippon. 1991;1(1):63-70.